Neuron
Article

# Fasting Activation of AgRP Neurons Requires NMDA Receptors and Involves Spinogenesis and Increased Excitatory Tone

Tiemin Liu,[1,4] Dong Kong,[1,4] Bhavik P. Shah,[1,4] Chianping Ye,[1,4] Shuichi Koda,[1,2] Arpiar Saunders,[3] Jun B. Ding,[3] Zongfang Yang,[1] Bernardo L. Sabatini,[3] and Bradford B. Lowell[1,*]
[1]Division of Endocrinology, Department of Medicine, Beth Israel Deaconess Medical Center and Harvard Medical School, Boston, MA 02115, USA
[2]Asubio Pharma Co., Ltd., Kobe 650-0047, Japan
[3]Howard Hughes Medical Institute, Department of Neurobiology, Harvard Medical School, Boston, MA 02115, USA
[4]These authors contributed equally to this work
*Correspondence: blowell@bidmc.harvard.edu
DOI 10.1016/j.neuron.2011.11.027

## SUMMARY

**AgRP neuron activity drives feeding and weight gain whereas that of nearby POMC neurons does the opposite. However, the role of excitatory glutamatergic input in controlling these neurons is unknown. To address this question, we generated mice lacking NMDA receptors (NMDARs) on either AgRP or POMC neurons. Deletion of NMDARs from AgRP neurons markedly reduced weight, body fat and food intake whereas deletion from POMC neurons had no effect. Activation of AgRP neurons by fasting, as assessed by c-Fos, *Agrp* and *Npy* mRNA expression, AMPA receptor-mediated EPSCs, depolarization and firing rates, required NMDARs. Furthermore, AgRP but not POMC neurons have dendritic spines and increased glutamatergic input onto AgRP neurons caused by fasting was paralleled by an increase in spines, suggesting fasting induced synaptogenesis and spinogenesis. Thus glutamatergic synaptic transmission and its modulation by NMDARs play key roles in controlling AgRP neurons and determining the cellular and behavioral response to fasting.**

## INTRODUCTION

Agouti-related peptide (AgRP)-expressing and proopiomelanocortin (POMC)-expressing neurons in the arcuate nucleus of the hypothalamus are important regulators of feeding and energy expenditure (Cone, 2005). AgRP neurons are anabolic (i.e., promote feeding and weight gain) whereas POMC neurons are catabolic. The evidence supporting these functions is very strong. Genetic ablation (Bewick et al., 2005; Gropp et al., 2005; Luquet et al., 2005; Xu et al., 2005) or pharmaco-genetic inhibition (Krashes et al., 2011) of AgRP neurons decreases food intake; optogenetic (Aponte et al., 2011) or pharmaco-genetic (Krashes et al., 2011) stimulation, on the other hand, drives intense food seeking behavior and feeding. In contrast, genetic ablation of POMC neurons (Xu et al., 2005) or gene knockout of *Pomc* (Smart et al., 2006; Yaswen et al., 1999), which encodes the protein precursor for the neuropeptide α-melanocyte stimulating hormone (αMSH), causes marked obesity; optogenetic stimulation, conversely, reduces food intake (Aponte et al., 2011). Finally, mice lacking the melanocortin-4 receptor (Balthasar et al., 2005; Huszar et al., 1997), which is antagonized and agonized, respectively, by AgRP and αMSH, develop massive obesity.

Given the important roles played by AgRP and POMC neurons, there is great interest in understanding the factors that regulate their activity. To date, most effort has been placed on examining direct regulation by various circulating, blood-borne factors such as leptin, insulin, and ghrelin (Belgardt et al., 2009; Castañeda et al., 2010; Friedman, 2009). The role of upstream neural inputs, on the other hand, has received comparatively less attention. This is surprising given that both AgRP and POMC neurons receive abundant excitatory and inhibitory synaptic input (Pinto et al., 2004; Sternson et al., 2005; van den Pol, 2003). Serotonergic tone provides additional regulation as evidenced by altered energy balance in mice with POMC neuron-specific manipulation of $5HT_{2c}$ receptors (Xu et al., 2008). GABAergic input is also likely to be important given that leptin, the adipocyte-secreted catabolic hormone, disinhibits POMC neurons by direct actions on presynaptic GABAergic neurons (Vong et al., 2011). Finally, as determined via laser scanning photostimulation in brain slices, POMC neurons receive glutamatergic input from neurons in the ventromedial nucleus of the hypothalamus (Sternson et al., 2005). In contrast, much less is known about neural afferent regulation of AgRP neurons. As assessed by electrophysiology (frequency of excitatory postsynaptic currents) and electron microscopy (presence of asymmetric synapses onto AgRP neuron somas), glutamatergic input is increased in mice with genetic deficiency of leptin (Pinto et al., 2004). In addition, in a recent report, it was shown that fasting activation of AgRP neurons is associated with increased frequency of excitatory postsynaptic currents (Yang et al., 2011). This was suggested to be caused by a ghrelin → ghrelin receptor → AMP-activated protein kinase pathway operating in presynpatic glutamatergic

neurons (Yang et al., 2011). In the present study, we investigate the physiologic significance of glutamatergic neurotransmission to AgRP and POMC neurons.

Rapid, excitatory neurotransmission is mediated by glutamatergic ionotropic AMPA (AMPARs) and NMDA receptors (NMDARs). Upon activation by glutamate, $Na^+$ enters via AMPARs, depolarizing the neuron, whereas $Ca^{2+}$ enters via NMDARs, engaging signaling pathways that modulate the strength/plasticity of glutamatergic transmission (Collingridge et al., 2010; Kessels and Malinow, 2009; Malenka and Nicoll, 1999). To evaluate the role of glutamatergic input to AgRP and POMC neurons, and more specifically its plasticity as regulated by NMDARs, we generated mice lacking NMDARs on either AgRP or POMC neurons. We accomplished this by crossing either *Agrp*-ires-Cre knockin mice (Tong et al., 2008) or *Pomc*-Cre BAC transgenic mice (Balthasar et al., 2004) with mice bearing loxed alleles of the *Grin1* gene (Tsien et al., 1996a). *Grin1* encodes NR1, a required subunit of the NMDAR. Consequently, deletion of *Grin1* causes total loss of NMDAR activity (Tsien et al., 1996b). Through such efforts, we have found that NMDARs on AgRP neurons, but not POMC neurons, play a critical role in controlling energy balance. Consistent with this, AgRP neurons, but not POMC neurons, have abundant dendritic spines, the postsynaptic specializations where most excitatory synapses reside and within which NMDARs operate to control plasticity (Bito, 2010; Higley and Sabatini, 2008; Yuste, 2010). Finally, fasting-mediated activation of AgRP neurons, which serves to promote food-seeking behavior and conservation of energy (Aponte et al., 2011; Krashes et al., 2011), is associated with markedly increased glutamatergic input, paralleled by and likely secondary to, at least in part, dendritic spinogenesis. Remarkably, the fasting-mediated increases in dendritic spines and glutamatergic neurotransmission, and the subsequent activation of AgRP neurons are all largely dependent upon the presence of postsynaptic NMDARs.

## RESULTS

### Deletion of *Grin1* in AgRP and POMC Neurons

*Agrp*$^{ires\text{-}Cre/+}$ knockin mice (Tong et al., 2008) and *Pomc*-Cre BAC transgenic mice (Balthasar et al., 2004) were crossed with lox-flanked *Grin1* mice (Jackson Labs 005246) (Tsien et al., 1996a) to disrupt NMDAR function in AgRP and POMC neurons. Control and *Grin1*-deleted study subjects were generated by mating *Grin1*$^{lox/lox}$ mice with either *Agrp*$^{ires\text{-}Cre/+}$, *Grin1*$^{lox/lox}$ mice or *Pomc*-Cre, *Grin1*$^{lox/lox}$ mice. The littermate offspring from such matings are either controls (i.e., *Grin1*$^{lox/lox}$ mice) or lack *Grin1* in AgRP (as in *Agrp*$^{ires\text{-}Cre/+}$, *Grin1*$^{lox/lox}$ mice) or POMC (as in *Pomc*-Cre, *Grin1*$^{lox/lox}$ mice) neurons. Cre-mediated deletion during early embryogenesis, secondary to "subthreshold" expression of Cre during very early development, occurs for some loxed alleles with *Agrp*-Cre BAC transgenic mice (Kaelin et al., 2004), and to a lesser degree with *Agrp*$^{ires\text{-}Cre}$ knockin mice (Tong et al., 2008). In the present study, early embryonic deletion of the *Grin1*$^{lox}$ allele was ruled out for all *Agrp*$^{ires\text{-}Cre/+}$, *Grin1*$^{lox/lox}$ study subjects (see Figure S1, available online, for details). In mice where brain slice electrophysiology was to be performed, *Npy*-hrGFP (van den Pol et al., 2009) or *Pomc*-hrGFP (Parton et al., 2007) BAC transgenes were crossed in for visualization of AgRP or POMC neurons. Of note, in the arcuate nucleus, NPY and AgRP are coexpressed in "AgRP" neurons (Broberger et al., 1998; Hahn et al., 1998). Consistent with this, hrGFP in the arcuate of *Npy*-hrGFP mice faithfully identifies AgRP neurons (van den Pol et al., 2009).

Electrophysiological analysis was performed in acute brain slices to confirm loss of NMDAR activity in neurons lacking *Grin1*. Electrically evoked EPSCs were recorded in the presence of low external $Mg^{2+}$ (to avoid $Mg^{2+}$-block of NMDARs) and picrotoxin (to block GABAA receptor-mediated IPSCs), and AMPAR and NMDAR components were subsequently isolated using D-APV to block NMDARs and CNQX to block AMPARs (see Experimental Procedures for details). The stimulus chosen for evoking AMPAR- and NMDAR-mediated EPSCs in each case was that which produced half maximal EPSC amplitudes within the linear region of the stimulation strength-peak amplitude curve. Deletion of *Grin1* in AgRP neurons (Figure 1A) or POMC neurons (Figure 1C) caused loss of evoked NMDAR-mediated EPSCs. We also assessed spontaneous EPSCs (in the presence of low external $Mg^{2+}$ and picrotoxin) and isolated AMPAR- and NMDAR-mediated components (Figures 1B and 1D). As was true for the evoked currents, spontaneous NMDAR-mediated EPSCs were absent (i.e., below the level of detection) in neurons lacking *Grin1* (Figure 1B, AgRP neurons; Figure 1D, POMC neurons). The above studies demonstrate, as anticipated based upon prior work (Tsien et al., 1996b), that NMDAR activity is absent in AgRP and POMC neurons lacking *Grin1*. Finally, deletion of *Grin1* in AgRP neurons did not significantly alter the frequency or, importantly, the amplitude of AMPAR-mediated spontaneous EPSCs (Figure 1B, right panel).

### Energy Balance in Mice Lacking *Grin1* in AgRP and POMC Neurons

Body weight and fat stores were markedly reduced in *Agrp*-ires-Cre, *Grin1*$^{lox/lox}$ mice (Figures 2A and 2B). This was due, at least in part, to reduced 24 hr ad libitum food intake (Figure 2C, left panel). Because fasting is known to activate AgRP neurons (Cone, 2005), we also assessed food intake following a 24 hr fast. As shown in Figure 2C (right panel), rates of refeeding were markedly decreased in *Agrp*-ires-Cre, *Grin1*$^{lox/lox}$ mice. Energy expenditure (as $O_2$ consumption) was measured (Figures S2A and S2B), but given the above-mentioned differences in body weight and body composition, which complicate normalization of $O_2$ consumption data (Butler and Kozak, 2010; Kaiyala and Schwartz, 2011), conclusions regarding its status cannot be drawn. Locomotor activity, which is a contributor to total energy expenditure, was normal in *Agrp*-ires-Cre, *Grin1*$^{lox/lox}$ mice (Figure S2C). Of interest, the respiratory exchange ratio ($CO_2$ exhaled ÷ $O_2$ inhaled), for which normalization issues are not a factor, was reduced in *Agrp*-ires-Cre, *Grin1*$^{lox/lox}$ mice (Figure 2D). This is consistent with preferential oxidation of lipid fuels in *Agrp*-ires-Cre, *Grin1*$^{lox/lox}$ mice.

Given that AgRP neurons promote feeding and weight gain, the observed reductions in body weight, fat stores, and food intake strongly suggest that AgRP neurons in *Agrp*-ires-Cre, *Grin1*$^{lox/lox}$ mice are less active. POMC neurons, on the other hand, are catabolic. If deletion of NMDARs were to similarly

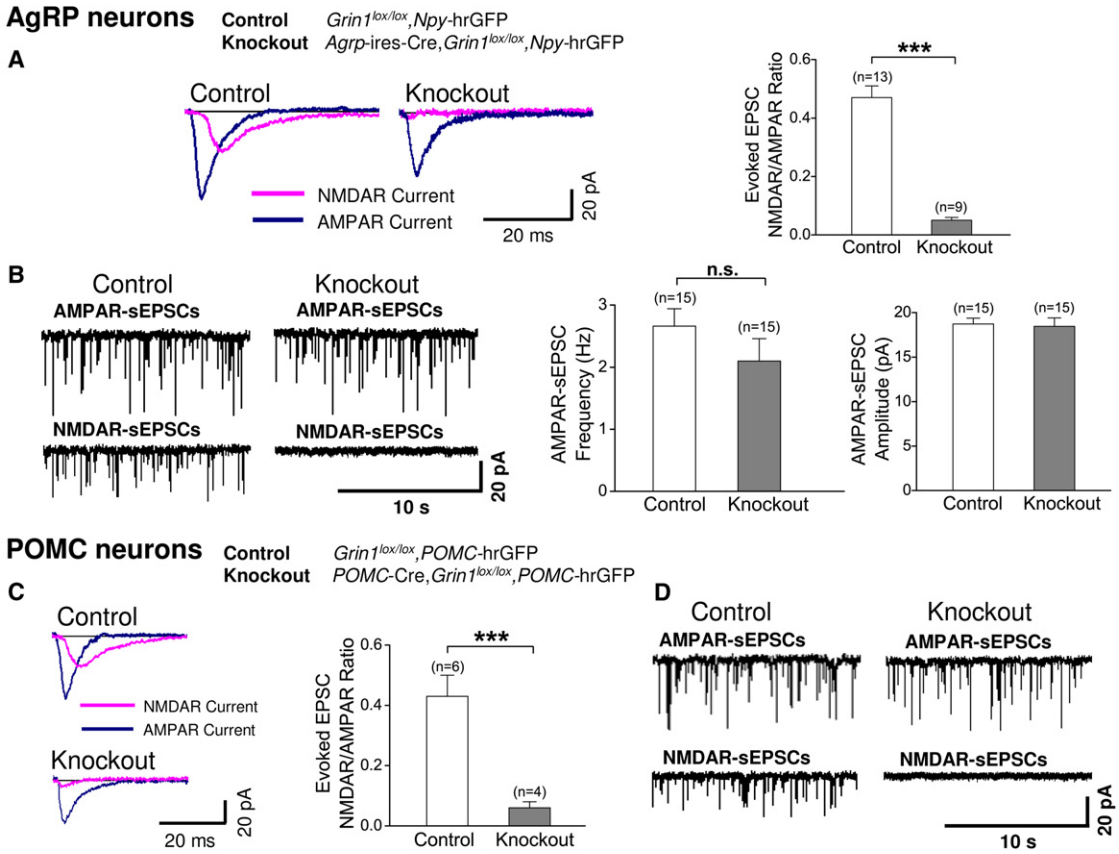


**Figure 1. Effects of *Grin1* Deletion on AMPAR- and NMDAR-Mediated Currents**

(A–D) Electrically-evoked (A and C) or spontaneous (B and D) AMPAR- and NMDAR-mediated EPSCs in AgRP neurons (A and B) and POMC neurons (C and D) within brain slices obtained from control (*Grin1*$^{lox/lox}$, *Npy*-hrGFP or *Grin1*$^{lox/lox}$, *Pomc*-hrGFP) mice and from *Grin1*-deleted (*Agrp*-ires-Cre, *Grin1*$^{lox/lox}$, *Npy*-hrGFP or *Pomc*-Cre, *Grin1*$^{lox/lox}$, *Pomc*-hrGFP) mice. (B) Right panels: quantitative analyses of AMPAR-sEPSC frequency and amplitude for control versus *Agrp*-ires-Cre, *Grin1*$^{lox/lox}$, *Npy*-hrGFP mice. Data are from male mice and are expressed as mean ± SEM. The number of GFP-positive neurons studied for each group is shown in parentheses. See also Figure S1.

reduce their activity, then *Pomc*-Cre, *Grin1*$^{lox/lox}$ mice should develop marked obesity. In contrast, body weight (Figure 2E), fat stores (Figure S2D), and food intake (Figure S2E) were essentially normal in *Pomc*-Cre, *Grin1*$^{lox/lox}$ mice. The marked phenotype caused by deletion of NMDARs in AgRP neurons, but not POMC neurons, strongly suggests that excitatory glutamatergic neurotransmission, and NMDAR-mediated control of its plasticity, plays a crucial role in regulating the activity of AgRP neurons but not POMC neurons.

## Presence and Absence of Dendritic Spines on AgRP and POMC Neurons

Given that in many brain areas most excitatory synapses are formed onto dendritic spines, we examined if AgRP and POMC neurons have dendritic spines. To accomplish this, we stereotaxically injected adeno-associated virus that conditionally expresses mCherry in the presence cre-recombinase (FLEX switch) (Schnütgen et al., 2003) into the arcuate nucleus of control mice (*Agrp*-ires-Cre mice or *Pomc*-Cre mice) or mice that lack *Grin1* in AgRP or POMC neurons (*Agrp*-ires-Cre, *Grin1*$^{lox/lox}$ mice and *Pomc*-Cre, *Grin1*$^{lox/lox}$ mice). We then obtained brain slices and performed confocal microscopy to ascertain the status of spines. As shown in Figures 3A and 3B, AgRP neurons have abundant dendritic spines whereas POMC neurons are essentially aspiny. Removal of NMDARs from AgRP neurons reduced the number of spines by ~50% and modestly decreased the spine head size and spine neck length, suggesting that NMDARs positively affect the number and size of spines.

## Effects of Fasting on c-Fos and Neuropeptide mRNAs

Fasting is known to activate AgRP neurons; therefore we examined if NMDARs are necessary for this activation. First, we tested the ability of fasting to induce c-Fos in AgRP neurons. This was accomplished by colocalizing immunodetectable c-Fos with hrGFP in *Npy*-hrGFP BAC transgenic mice which marks the AgRP neurons. As shown in Figure 4A, fasting doubled the percentage of AgRP neurons expressing c-Fos. Of note, this fasting-induced increase in c-Fos was diminished in *Agrp*-ires-Cre, *Grin1*$^{lox/lox}$ mice. Next, we assessed the effects of fasting on *Agrp*, *Npy*, and *Pomc* mRNA levels in the medial basal hypothalamus. Confirming what has been observed by others

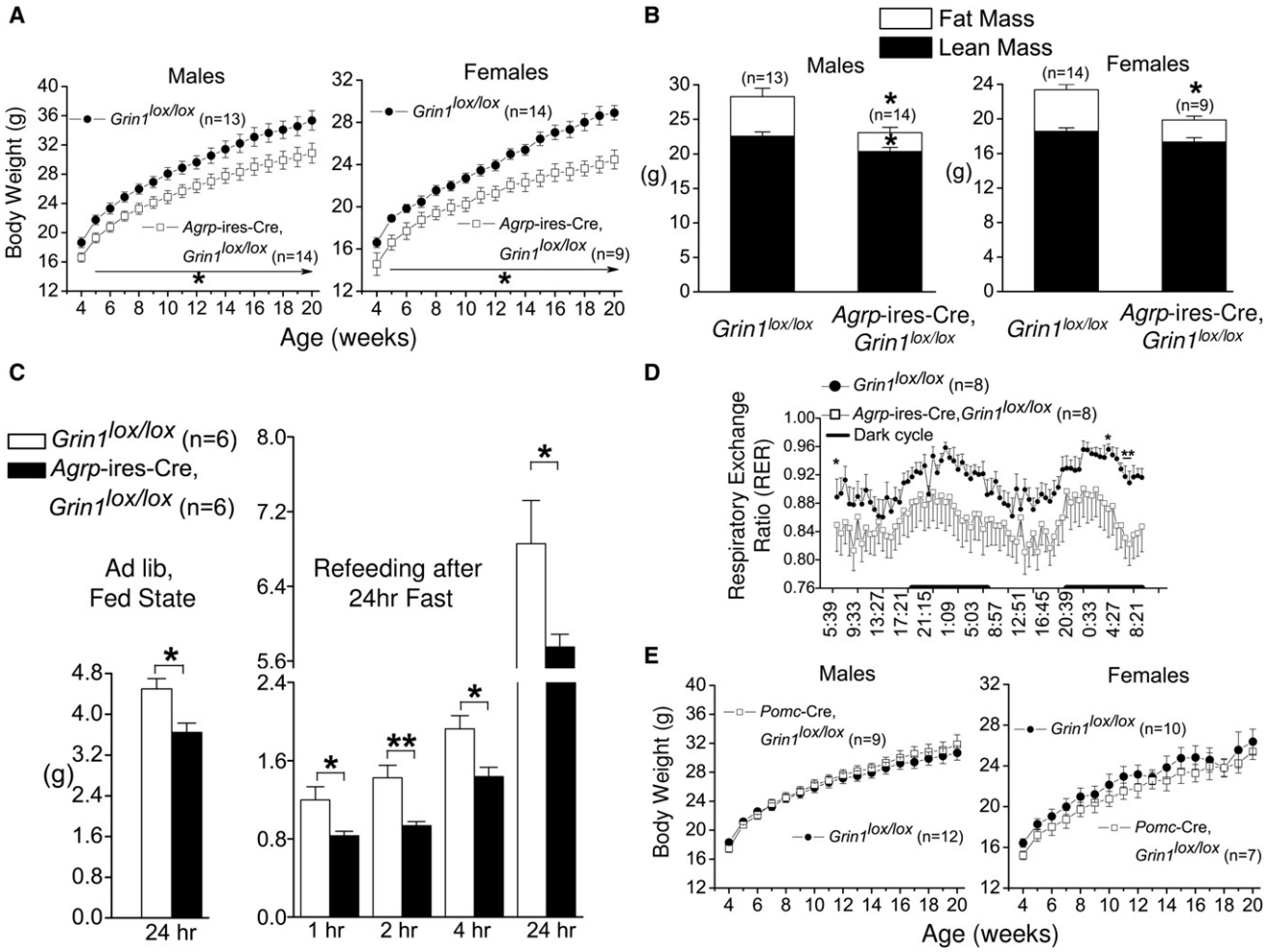


**Figure 2. Effects of *Grin1* Deletion on Energy Balance**

(A–D) Body weight (A) (males and females), body composition (B) (males and females), food intake (C) (males, ad libitum [left] and 24 hr fasted-refeeding [right]), and respiratory exchange ratio (D) (males) of control (*Grin1*$^{lox/lox}$) mice and AgRP neuron-specific, *Grin1*-deleted (*Agrp*-ires-Cre, *Grin1*$^{lox/lox}$) mice.

(E) Body weight (males and females) of control (*Grin1*$^{lox/lox}$) mice and POMC neuron-specific, *Grin1*-deleted (*Pomc*-Cre, *Grin1*$^{lox/lox}$) mice. Data are expressed as mean ± SEM. *$p < 0.05$, **$p < 0.01$, unpaired t test compared to controls. The number of mice studied for each group is shown in parentheses. See also Figure S2.

(reviewed in Cone, 2005), fasting increased the expression of *Agrp* and *Npy* mRNAs, and decreased the expression of *Pomc* mRNA (Figures 4B–4D). Of importance, the fasting-mediated increase in *Agrp* and *Npy* mRNAs, which are both expressed in the AgRP neurons, but not the fasting-mediated fall in *Pomc* mRNA, which is expressed in the POMC neurons, was greatly attenuated in *Agrp*-ires-Cre, *Grin1*$^{lox/lox}$ mice. Combined, the marked impairments in fasting-induced c-Fos, and *Agrp* and *Npy* mRNA expression caused by deletion of NMDARs, demonstrate that activation of AgRP neurons by fasting is largely dependent upon the presence of NMDARs. In contrast, but consistent with the lack of phenotype in *Pomc*-Cre, *Grin1*$^{lox/lox}$ mice, the fasting-mediated fall in *Pomc* mRNA, and parenthetically the fasting-mediated increase in *Agrp* and *Npy* mRNAs, were unaffected by deletion of NMDARs from POMC neurons (Figures 4B–4D). To summarize, the fasting-mediated activation of AgRP neurons, but not the fasting-mediated inhibition of POMC neurons, is dependent upon the presence of NMDARs.

## Effects of Fasting on Number of Dendritic Spines

Given the importance of NMDARs in fasting-mediated activation of AgRP neurons and in determining the density of dendritic spines on AgRP neurons, we investigated if fasting alters dendritic spine number. This possibility is of interest because spine numbers are plastic in the hypothalamus (Csakvari et al., 2007; Frankfurt et al., 1990) and spinogenesis in other brain regions is dependent upon NMDARs (Engert and Bonhoeffer, 1999; Kwon and Sabatini, 2011; Maletic-Savatic et al., 1999). Of note, 24 hr of fasting markedly increased spine number on AgRP neuron dendrites (by 67%) (Figure 5). Importantly, and consistent with the requirement for NMDARs in fasting-mediated activation of AgRP neurons noted earlier, this stimulatory effect on spine number was greatly attenuated in mice lacking

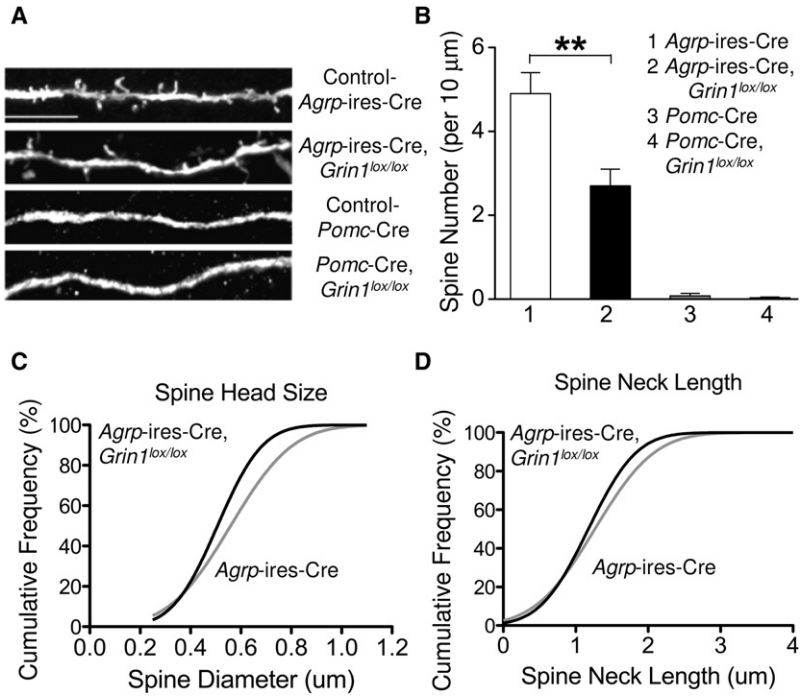


**Figure 3. Dendritic Spines on AgRP and POMC Neurons**

(A and B) Visualization (A) and quantification (B) of spines on dendrites of AgRP and POMC neurons in control (*Agrp*-ires-Cre or *Pomc*-Cre, respectively) and neuron-specific, *Grin1*-deleted (*Agrp*-ires-Cre, *Grin1*$^{lox/lox}$, or *Pomc*-Cre, *Grin1*$^{lox/lox}$) mice. Scale bar in (A) represents 10 μm.

(C and D) Determination of head size (C) and neck length (D) of spines on dendrites of AgRP neurons in control (*Agrp*-ires-Cre) and AgRP neuron-specific, *Grin1*-deleted (*Agrp*-ires-Cre, *Grin1*$^{lox/lox}$) mice. Data for each group was collected from n = 3 male mice (seven to nine neurons per mouse) and are expressed as mean ± SEM. **p < 0.01, unpaired t test compared to controls.

NMDARs on AgRP neurons. These findings suggest that dendritic spinogenesis, which requires the presence of NMDARs, plays an important role in fasting-mediated activation of AgRP neurons.

## Effects of Fasting on Electrophysiology of AgRP Neurons

We next determined if the fasting-induced increase in spines translates into increased synaptic transmission and excitability of AgRP neurons, and, if so, whether these effects are also dependent on NMDARs. We first evaluated the effects of fasting on AMPAR-mediated synaptic input to AgRP neurons. Fasting doubled the frequency, but had no effect on the amplitude, of AMPAR-isolated spontaneous (Figure 6A) and miniature (Figure 6B) EPSCs (AMPAR-sEPSCs and AMPAR-mEPSCs, respectively). This finding is very similar to a recently published observation (Yang et al., 2011). An increase in frequency without any increase in amplitude is consistent with an increase in active synapse number, a possibility that is likely given the fasting-mediated increase in dendritic spines. Of note, the fasting-induced doubling in AMPAR-EPSC frequencies, similar to the increase in spines, was absent in brain slices from mice lacking postsynaptic NMDARs on AgRP neurons (Figure 6). These findings are consistent with the possibility that the fasting-mediated increase in glutamatergic input is caused, at least in part, by the increase in dendritic spines and the increase in excitatory synapses that is expected to accompany it.

The fasting-induced increase in EPSC frequency could also be caused by increased presynaptic release. To test if fasting increases presynaptic release probability, we assessed paired-pulse ratios (PPR = P2/P1) (Xu-Friedman and Regehr, 2004) in slices from fed and fasted *Npy*-hrGFP mice. Glutamatergic input to AgRP neurons demonstrated paired-pulse depression and this was unaffected by fasting (PPR, mean ± SEM, fed = 0.67 ± 0.04, n = 23; fasted = 0.66 ± 0.05, n = 20) (Figure S3). This lack of effect on PPR suggests that increased EPSC frequency with fasting is not secondary to changes in presynaptic release.

To investigate the influence of NMDAR-dependent regulation of glutamatergic input on excitability, we next assessed membrane potentials and firing rates of AgRP neurons (Figure 7). Fasting depolarized and markedly increased the firing rate of AgRP neurons. Note, a stimulatory effect of fasting on firing rate of AgRP neurons has previously been observed (Takahashi and Cone, 2005; Yang et al., 2011). Importantly, and consistent with the findings presented above, the fasting-induced depolarization and increase in firing rates was absent in brain slices from mice lacking NMDARs on AgRP neurons (Figure 7). Of note, the fasting-mediated increases in glutamatergic input (Figure 6) and excitation (Figure 7) of AgRP neurons are congruent with, and likely account for, the requirement for NMDARs in the fasting-mediated increases in c-Fos, *Agrp* and *Npy* mRNA in AgRP neurons, as well as the impairment in refeeding following fasting in *Agrp*-ires-Cre, *Grin1*$^{lox/lox}$ mice.

## Reversibility of Fasting-Induced Changes in EPSCs and Spines

Mice were fasted for 24 hr and then refed for up to 3 days to assess the reversibility, as well as the time course of reversibility, for fasting-induced changes in sEPSC frequency and dendritic spinogenesis. Following fasting, food intake was significantly elevated above ad libitum levels for up to 2 days, ultimately returning to normal by the third day of refeeding (Figure 8A). In agreement with our earlier results (shown in Figure 5 and Figure 6), fasting increased both EPSC frequency (Figure 8B) and the number of dendritic spines (Figure 8C). Following 3 days of refeeding, EPSC frequency and spine number both returned to normal in agreement with the normalization of food intake. Of note, following 1 day of refeeding when food intake remained elevated, sEPSC frequency and the number of spines were both intermediate between the elevated levels seen in fasted mice

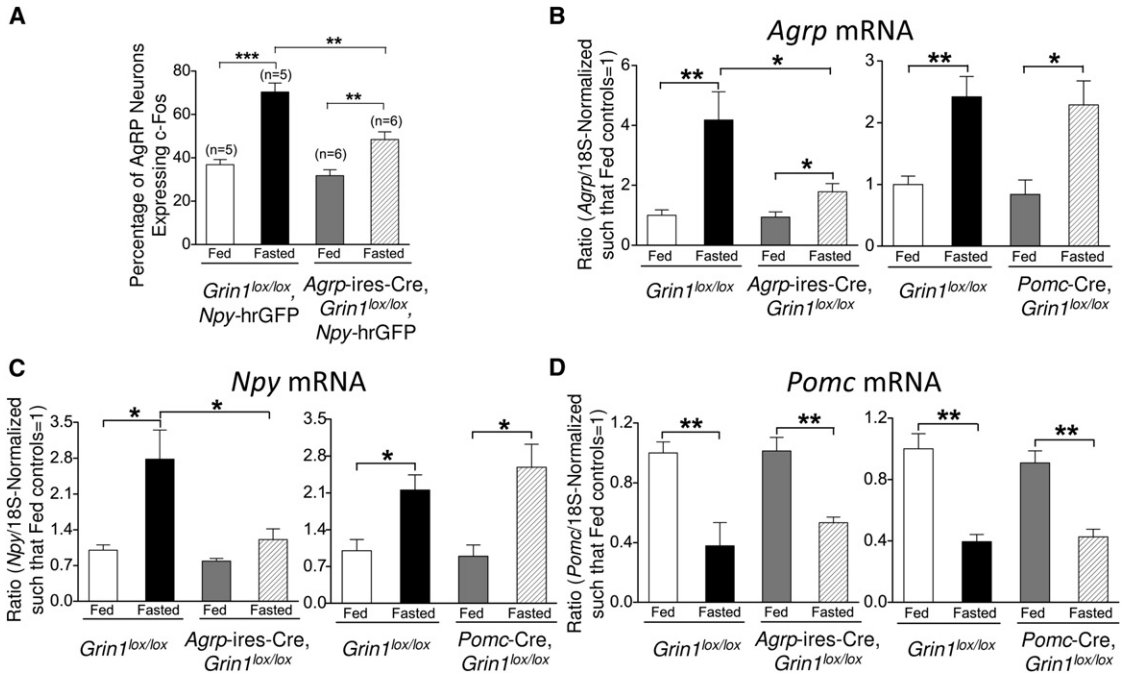


**Figure 4. Fasting-Induced Increases in c-Fos Protein and Neuropeptide mRNAs in AgRP Neurons—Dependence on NMDARs**

(A) Effects of fasting on c-Fos induction in AgRP neurons of control (*Grin1*$^{lox/lox}$, *Npy*-hrGFP) mice and AgRP neuron-specific, *Grin1*-deleted (*Agrp*-ires-Cre, *Grin1*$^{lox/lox}$, *Npy*-hrGFP) mice. The number of mice studied for each group is shown in parentheses.

(B–D) Effects of fasting on *Agrp* (B), *Npy* (C), and *Pomc* (D) mRNA expression in hypothalami of control (*Grin1*$^{lox/lox}$) mice, AgRP neuron-specific, *Grin1*-deleted (*Agrp*-ires-Cre, *Grin1*$^{lox/lox}$) mice and POMC neuron-specific, *Grin1*-deleted (*Pomc*-Cre, *Grin1*$^{lox/lox}$) mice. For (B–D), the number of mice studied for each group is greater than or equal to four. Data are from male mice and are expressed as mean ± SEM. *$p < 0.05$, **$p < 0.01$, ***$p < 0.001$, one-way ANOVA followed by Tukey's HSD post-hoc test compared to controls as indicated in the figure.

and the normal levels observed after 3 days of refeeding. The fact that dendritic spine number increases with fasting and then decreases with refeeding, with a time course that is similar to the changes observed in EPSC frequency and feeding, suggests strongly that changes in spine number, and likely the number of functional synapses, play key roles in fasting-induced increases in EPSC frequency and also fasting-induced, AgRP neuron-driven feeding.

## DISCUSSION

In the present study, we have investigated the role of glutamatergic excitatory input, specifically, the modulation of its plasticity by NMDARs, in regulating the activity and function of AgRP and POMC neurons. Strikingly, deletion of NMDARs from AgRP neurons caused marked reductions in body weight, fat mass, ad lib food intake and fasted-induced refeeding; consequences that are expected to follow decreased activity of AgRP neurons. In sharp contrast, deletion of NMDARs from POMC neurons produced no changes in body weight, fat mass, or food intake, consistent with NMDARs playing little or no role in POMC neuron-mediated regulation of feeding and energy balance, at least under the normal housing and diet conditions employed in this study. If activity of POMC neurons had been reduced, as occurred with AgRP neurons, then *Pomc*-Cre, *Grin1*$^{lox/lox}$ mice would have developed marked obesity because prior studies have established that the function of POMC neurons is to limit weight gain (Aponte et al., 2011; Smart et al., 2006; Xu et al., 2005; Yaswen et al., 1999). Of interest, and in agreement with the important role of NMDARs on AgRP but not POMC neurons, we have found that AgRP neurons have abundant dendritic spines whereas POMC neurons, on the other hand, are essentially aspiny. The presence/absence of spines on AgRP versus POMC neurons could account for, or is at least likely related to, the plasticity-inducing, activity-regulating effects of NMDARs on AgRP neurons. This is because these specialized, femtoliter-order protrusions, along with the elaborate signaling pathways that are confined within, provide the neurobiological substrate for modulation of glutamatergic neurotransmission (Bito, 2010; Higley and Sabatini, 2008; Yuste, 2010).

### Role of NMDARs/Dendritic Spines in Fasting Activation of AgRP Neurons

Fasting is known to increase the activity of AgRP neurons (reviewed in Cone, 2005). This response is likely to be important because optogenetic (Aponte et al., 2011) and pharmacogenetic (Krashes et al., 2011) stimulation of AgRP neurons drives intense food-seeking behavior, increased feeding and expansion of fat stores, whereas genetic ablation (Bewick et al., 2005; Gropp et al., 2005; Luquet et al., 2005; Xu et al., 2005) or pharmaco-genetic inhibition (Krashes et al., 2011) of AgRP

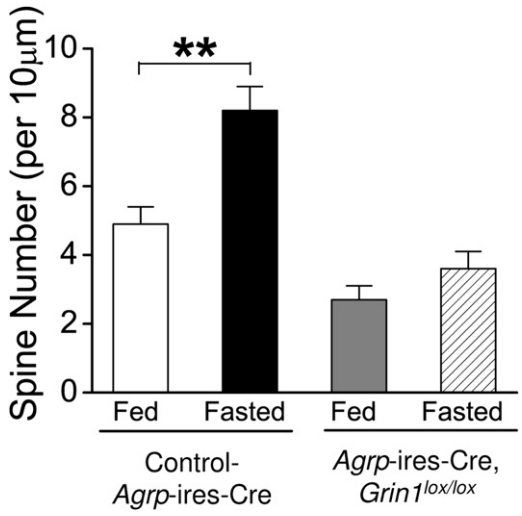


**Figure 5. Fasting-Induced Increase in Dendritic Spines—Dependence on NMDARs**

Effects of fasting on number of spines on AgRP neuron dendrites in control (*Agrp*-ires-Cre) mice and in AgRP neuron-specific, *Grin1*-deleted (*Agrp*-ires-Cre, *Grin1*$^{lox/lox}$) mice. Data for each group was collected from n = 3 male mice (seven to nine neurons per mouse) and are expressed as mean ± SEM. **p < 0.01, unpaired t test compared to controls. Note, data shown in this figure for the two fed groups was previously presented in Figure 3B (labeled as 1 *Agrp*-ires-Cre and 2 *Agrp*-ires-Cre, *Grin1*$^{lox/lox}$ in that figure) and is shown here again to permit comparison with the fasted groups.

neurons reduces food intake. Remarkably, fasting-induced changes in AgRP neurons, such as increased c-Fos, *Npy*, and *Agrp* mRNAs, depolarization and increased firing rates, are all completely, or largely, in the case of c-Fos and *Npy* and *Agrp* mRNAs, dependent upon the presence of NMDARs on AgRP neurons (i.e., are absent or are greatly reduced in *Agrp*-ires-Cre, *Grin1*$^{lox/lox}$ mice). Similarly, the fasting-induced augmentation of glutamatergic input to AgRP neurons, demonstrated by a 2-fold increase in the frequency of AMPAR-mediated spontaneous and miniature EPSCs, is also entirely dependent upon the presence of NMDARs. Given this, we favor the view that the fasting-induced increase in glutamatergic input drives the other fasting-related responses, specifically the increases in c-Fos, *Npy*, and *Agrp* mRNAs, depolarization and increases in firing rate. This would account for the NMDAR-dependence of each of these diverse responses.

What then is responsible for the fasting-induced increase in glutamatergic input? Given that it is paralleled by an increase in dendritic spines, it is likely that dendritic spinogenesis, and the acquisition of new synapses that is expected to accompany it, plays an important role. The following three findings support this view. First, the increase and subsequent decrease in spine number with fasting and refeeding parallels the observed changes in EPSC frequency. Second, and importantly, fasting-induced spinogenesis, like the increased glutamatergic input, is similarly dependent upon the presence of NMDARs. Third, the fasting-induced increase in AMPAR-EPSC frequency occurs without any change in amplitude, which is consistent with an increase in synapse number.

Of note, two alternative explanations are possible for increased frequency without any change in amplitude and include increased release from presynaptic terminals, as recently suggested (Yang et al., 2011), and/or postsynaptic unsilencing of glutamatergic synapses (Kerchner and Nicoll, 2008). We do not favor a presynaptic mechanism for the following three reasons: 1), fasting did not alter the paired-pulse ratio (Figure S3); 2), postsynaptic NMDARs are required for the fasting increase in EPSC frequency (Figure 6); and finally, 3), importantly, the fasting increase in EPSC frequency is paralleled by dendritic spinogenesis, a harbinger for excitatory synaptogenesis, which is expected to cause increased frequency of EPSCs. Postsynaptic unsilencing, which could be affected by NMDARs, has to our knowledge not yet been reported in hypothalamic circuits. Although we are unable to exclude a role for these two alternative possibilities, and they may indeed be operating to a degree concurrently with the structural changes that we have observed, we favor the view, as stated above, that increased glutamatergic input brought about by fasting is caused, in large part, by dendritic spinogenesis and the expected increase in synapse number. Consistent with this, prior studies have shown spinogenesis to be modulated in the hypothalamus (Csakvari et al., 2007; Frankfurt et al., 1990) and, as will be discussed in a subsequent section, in other brain sites to be dependent upon NMDARs (Engert and Bonhoeffer, 1999; Kwon and Sabatini, 2011; Maletic-Savatic et al., 1999).

With regards to fasting-induced spinogenesis and the possibility of new synapses, it is interesting to note that leptin treatment of leptin-deficient (*Lepr*$^{ob/ob}$) mice, which have at baseline many more excitatory synapses on the perikarya of AgRP neurons, quickly, within 6 hr of treatment, reduces synapse number (Pinto et al., 2004). This rapid capacity for reorganization of synapses on AgRP neurons is of interest and could be related, in some way, to our findings involving dendritic spines. The nature of this relationship, however, is uncertain because the EM-detected excitatory synapses (Pinto et al., 2004) were on perikarya and not on dendritic spines.

To summarize up to this point, we have put forth the following tentative model to account for fasting-mediated activation of AgRP neurons: fasting → dendritic spinogenesis → formation of new excitatory synapses → increased glutamatergic transmission → activation of AgRP neurons. In support of this view, we have observed that the increase in dendritic spines, an early step in the proposed model, requires postsynaptic NMDARs, a "plasticity-driving" receptor activated by glutamate. This then raises the distinct possibility that presynpatic release of glutamate, which then engages postsynaptic NMDARs on AgRP neurons, somehow initiates the spinogenesis. Consistent with this, previous studies have found that dendritic spinogenesis occurs in response to evoked synaptic glutamate release (Engert and Bonhoeffer, 1999; Maletic-Savatic et al., 1999) and also, very rapidly, following focal glutamate uncaging onto dendritc shafts (Kwon and Sabatini, 2011). As was true with fasting, these studies similarly found a requirement for NMDARs. Combined, these observations suggest that glutamatergic afferents to AgRP neurons are very likely to play important roles in activating AgRP neurons—in promoting spinogenesis via release of glutamate that then engages NMDARs on AgRP neurons, in providing

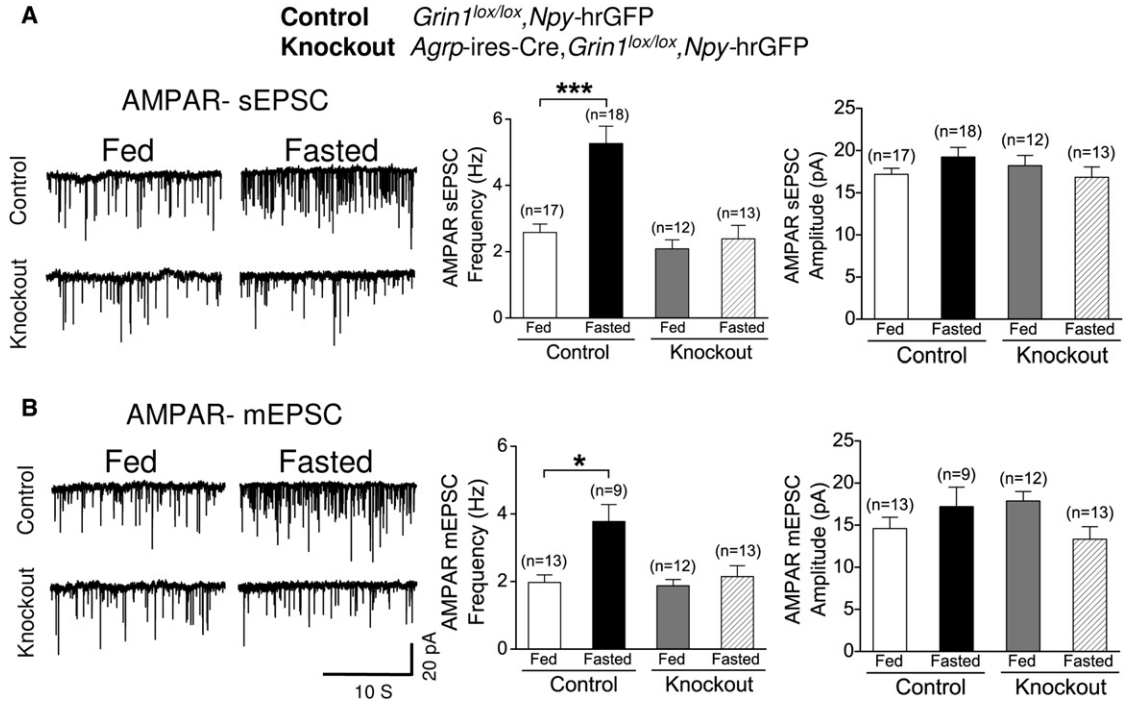


**Figure 6. Fasting-Induced AMPAR-Mediated EPSCs in AgRP Neurons—Dependence on NMDARs**

(A and B) Effects of fasting on AMPAR-mediated EPSC frequencies and amplitudes (spontaneous EPSCs [A] and miniature EPSCs [B]) in AgRP neurons within brain slices obtained from control (*Grin1*$^{lox/lox}$, *Npy*-hrGFP) mice and from AgRP neuron-specific, *Grin1*-deleted (*Agrp*-ires-Cre, *Grin1*$^{lox/lox}$, *Npy*-hrGFP) mice. Representative traces are shown in the left panels of (A) and (B). Data are from male mice and are expressed as mean ± SEM. *p < 0.05, ***p < 0.001, unpaired t test compared to controls. The number of GFP-positive neurons studied for each group is shown in parentheses. See also Figure S3.

presynaptic partners for the new dendritic spines and, finally, in providing sustained activation of the nascent synapses.

## Implications of NMDARs/Spines on AgRP Neurons

The marked effects caused by removing NMDARs from AgRP neurons reviewed above, in combination with the presence of dendritic spines on AgRP neurons but not on nearby POMC neurons, strongly suggests that glutamatergic neurotransmission, and its regulation via NMDARs, along with signaling events that are confined within dendritic spines, play key roles in regulating the activity of AgRP neurons. Dendritic spines, and the signaling within, serve three major functions, and each of these has important implications for mechanisms regulating AgRP neurons and feeding behavior. First, spines are the sites where excitatory afferents are received. Given that AgRP neurons drive feeding behavior (Aponte et al., 2011; Krashes et al., 2011), these excitatory afferents must, by extension, be key, but presently unknown, drivers of food intake. Identifying these excitatory afferents should shed new light on neural circuits regulating feeding. Second, NMDARs/spines are mediators of plasticity (i.e., changes in strength of glutamatergic transmission). Given this, it is likely that mechanisms of plasticity, including long term potentiation, long term depression, and dendritic spinogenesis (Collingridge et al., 2010; Engert and Bonhoeffer, 1999; Kessels and Malinow, 2009; Kwon and Sabatini, 2011; Malenka and Nicoll, 1999; Maletic-Savatic et al., 1999), play important roles in controlling feeding behavior.

Third, and of special relevance to hypothalamic neurons, dendritic spines serve as communication hubs where other "inputs" are integrated for the purpose of acutely and chronically modulating glutamatergic transmission. Notable examples of this include dopaminergic and cholinergic modulation, respectively, of glutamatergic transmission in the striatum (Kreitzer and Malenka, 2008) and hippocampus (Buchanan et al., 2010; Giessel and Sabatini, 2010). It is likely that related forms of modulation occur within the spines of AgRP neurons. Modulatory input could come from release of other neurotransmitters, as in the examples noted above, and/or of great relevance to neurons in the arcuate nucleus where access to blood-borne factors is excellent, from various circulating hormones. One interesting possibility is ghrelin, a fasting-induced, orexigenic hormone that is known to activate AgRP neurons (Castañeda et al., 2010; Cowley et al., 2003) and to affect dendritic spines (Diano et al., 2006). Identifying the neurotransmitters along with their sources and, importantly, the hormones that modulate glutamatergic transmission to AgRP neurons, and the mechanisms by which this modulation occurs, is likely to provide a neurobiologic, mechanistic understanding of how various factors control feeding behavior.

## EXPERIMENTAL PROCEDURES

### Animal Studies

#### *Animal Care*

Care of all animals and procedures were approved by the Beth Israel Deaconess Medical Center Institutional Animal Care and Use Committee.

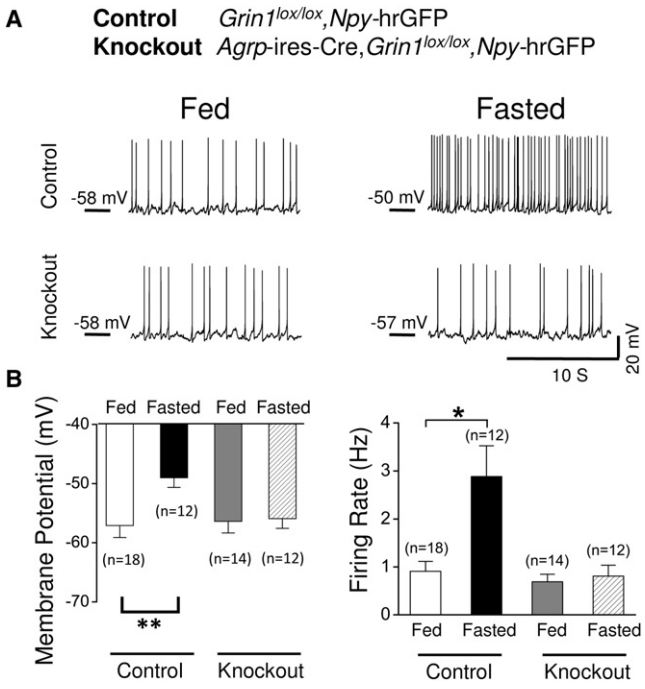


**Figure 7. Fasting-Induced Depolarization and Firing Rates in AgRP Neurons—Dependence on NMDARs**

(A and B) Effects of fasting on membrane potential and firing rate of AgRP neurons within brain slices obtained from control (*Grin1*$^{lox/lox}$, *Npy*-hrGFP) mice and from AgRP neuron-specific, *Grin1*-deleted (*Agrp*-ires-Cre, *Grin1*$^{lox/lox}$, *Npy*-hrGFP) mice. Representative traces are shown in (A). (B) Bar graph summaries of membrane potential (left) and firing rate (right). Data are from male mice and are expressed as mean ± SEM. *p < 0.05, **p < 0.01, unpaired t test compared to controls. The number of GFP-positive neurons studied for each group is shown in parentheses.

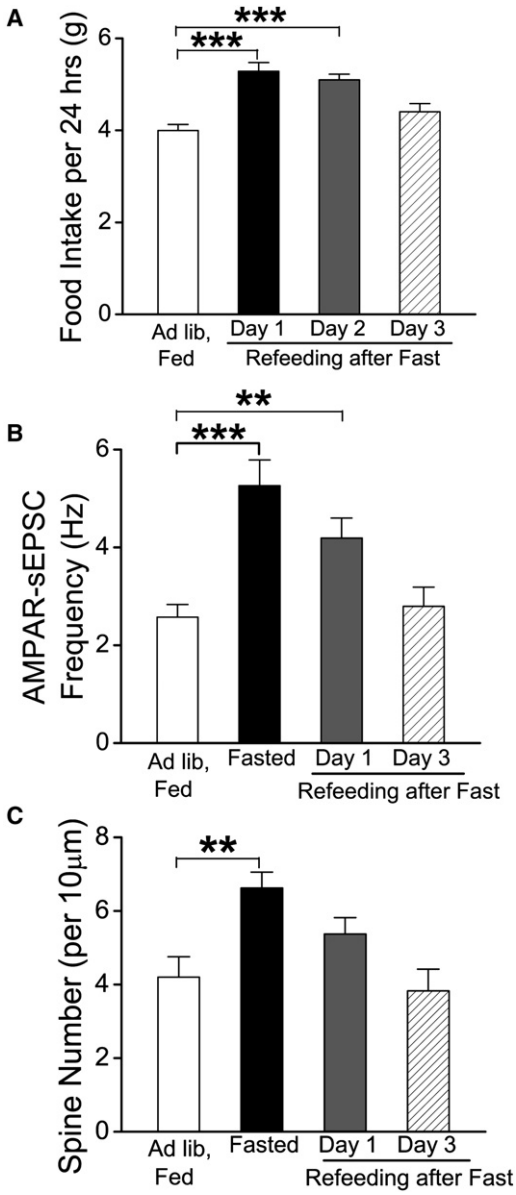


**Figure 8. Reversibility of Fasting-Induced Changes in EPSCs and Spines**

(A) Daily food intake in male *Npy*-hrGFP mice that were ad libitum fed, then fasted for 24 hr, and then refed for 3 days. Data for each group was collected from n ≥ 3 male mice.

(B) Effects of fasting and refeeding on AMPAR-mediated spontaneous EPSC frequencies in AgRP neurons within brain slices obtained from male *Npy*-hrGFP mice. The number of GFP-positive neurons studied ranges from 14–18 in each group.

(C) Effects of fasting and refeeding on the number of spines on AgRP neuron dendrites in male *Agrp*-ires-Cre mice. Spines were counted using methods identical to those employed for data in Figures 3 and 5. Spine data for each group was collected from three mice (seven to nine neurons per mouse). Data in (A–C) are expressed as mean ± SEM with **p < 0.01, ***p < 0.001, one-way ANOVA followed by Tukey's HSD post-hoc test compared to ad lib fed controls.

Unless otherwise specified, mice were housed at 22°C–24°C using a 12 hr light/12 hr dark cycle with ad libitum access to standard pelleted mouse chow (Teklad F6 Rodent Diet 8664, 12.5% kcal from fat; Harlan Teklad, Madison, WI) and water.

### *Genetically Engineered Mice*

The mice used in this study are shown below along with their original references and Jackson Laboratory stock numbers: *Agrp*$^{ires\text{-}Cre/+}$ knockin mice (#012899) (Tong et al., 2008), *Pomc*-Cre BAC transgenic mice (#005965) (Balthasar et al., 2004), lox-flanked *Grin1* mice (#005246) (Tsien et al., 1996a), *Npy*-hrGFP BAC transgenic mice (#006417) (van den Pol et al., 2009) and *Pomc*-hrGFP BAC transgenic mice (#006421) (Parton et al., 2007). The lox-flanked *Grin1* mice were obtained from Jackson Labs. All other mice were from our mouse colony at Beth Israel Deaconess Medical Center where they originated. Breeding strategies are as described in Results.

### *Body Composition*

Total fat and lean mass were analyzed using the EchoMRI system (Echo Medical Systems).

### *Food Intake*

Male mice were singly housed for at least 2 weeks prior to assessing food intake. For the fasting-refeeding studies, food was removed and then replaced, 24 hr later, at 9 AM (at the start of the "lights-on" cycle). Food intake was then assessed over the ensuing 1, 2, 3, and 24 hr.

### *Energy Expenditure, Respiratory Exchange Ratio, and Locomotor Activity*

These parameters were measured in male mice using the Comprehensive Lab Animal Monitoring System (CLAMS, Columbus Instruments, Columbus, OH).

Mice were acclimated in the chambers for 48 hr prior to data collection. Mice had free access to food and water during these studies.

#### Stereotaxic Injection of AAV for Assessment of Spine Morphology

Four-week-old *Agrp*$^{ires\text{-}Cre/+}$ mice or *Pomc*-Cre BAC transgenic mice were stereotaxically injected with cre-dependent AAV-DIO-mCherry (see below for details of virus), unilaterally, using techniques that have previously been described (Krashes et al., 2011). The injections were aimed at the arcuate nucleus (coordinates, bregma: anterior-posterior, –1.40 mm; dorsal-ventral, –5.80 mm; lateral, ±0.30 mm).

#### Tissue Collection for Histology

Animals were deeply anesthetized by intraperitoneal injection of chloral hydrate (500 mg/kg per mouse) and subsequently perfused transcardially with diethylpyrocarbonate (DEPC)-treated, 0.9% phosphate buffered saline (PBS) followed by 10% neural buffered formalin. Brains were removed, stored in the same fixative for 4–6 hr at 4°C, transferred to a 20% sucrose DEPC-treated PBS, pH 7 at 4°C overnight, and cut into 30 μm coronal sections on a microtome.

### Electrophysiology Studies

#### Slice Preparation and Whole-Cell Recordings

Brain slices were prepared from young adult male mice (5–7-week-old) as previously described (Dhillon et al., 2006; Vong et al., 2011). Briefly, 300 μM thick coronal sections were cut with a Leica VT1000S vibratome and then incubated in carbogen-saturated (95% $O_2$/5% $CO_2$) aCSF at room temperature for at least 1 hr before recording. Slices were transferred to the recording chamber perfused with aCSF (in mM: 126 NaCl, 2.5 KCl, 1.2 $MgCl_2$, 2.4 $CaCl_2$, 1.2 $NaH_2PO_4$, 21.4 $NaHCO_3$, 10 glucose) at a flow rate of ~2 ml/min. The slices were allowed to equilibrate for 10–20 min before performing whole-cell recordings. All electrophysiology recordings were performed at room temperature.

#### Evoked AMPAR-Mediated and NMDAR-Mediated EPSCs

To verify the deletion of NMDARs in AgRP neurons or POMC neurons, we performed whole-cell, voltage-clamp recordings in the presence of low $Mg^{2+}$ ($MgCl_2$ in aCSF was reduced from 1.2 mM to 0.1 mM) to avoid $Mg^{2+}$-block of NMDARs, and 100 μM picrotoxin (PTX) to block GABAA receptor-mediated IPSCs. A stimulating electrode was placed near the VMH 300–500 μm from the recording electrode. Excitatory postsynaptic currents were evoked by 0.1 Hz stimulation. The stimulation strength chosen for evoking AMPAR- and NMDAR-mediated EPSCs in each case was to produce half maximal EPSC amplitudes within the linear region of the stimulation strength-peak amplitude curve. The evoked NMDAR- or AMPAR-mediated currents were constructed by averaging 12 EPSCs elicited at −60 mV. NMDA currents were calculated by subtracting the average response in the presence of 50 μm D-APV from that recorded in its absence. AMPA current was then calculated by subtracting the background currents (recorded in the presence of 50 μm D-APV and 30 μm CNQX) from that recorded in the presence of D-APV only.

#### Excitatory Postsynaptic Currents

EPSCs were measured in whole-cell voltage-clamp mode with a holding potential of −60 mV. The internal recording solution contained (in mM): $CsCH_3SO_3$ 125; CsCl 10; NaCl 5; $MgCl_2$ 2; EGTA 1; HEPES 10; (Mg)ATP 5; (Na)GTP 0.3 (pH 7.35 with NaOH). Currents were amplified, filtered at 1 kHz, and digitized at 20 kHz. EPSCs were measured in the presence of 100 μM picrotoxin (PTX). Miniature EPSCs were recorded with 1 μm tetrodotoxin in aCSF recording solution. Frequency and peak amplitude were measured by using the Mini Analysis program (Synaptosoft).

#### Membrane Potential and Firing Rate

Membrane potential and firing rate were measured by whole-cell current clamp recordings from AgRP neurons in brain slices. Recording electrodes had resistances of 2.5–4 MΩ when filled with the K-gluconate internal solution (128 mM K-gluconate, 10 mM HEPES, 1 mM EGTA, 10 mM KCl, 1 mM $MgCl_2$, 0.3 mM $CaCl_2$, 3 mM Mg-ATP, and 0.3 mM Na-GTP, pH 7.35 with KOH). Liquid junction potential correction was performed off-line.

#### Paired-Pulse Ratio

Paired-pulse ratio (PPR) experiments were carried out to estimate release probability. The peak amplitude of excitatory postsynaptic currents (EPSCs) evoked by two identical electrical stimuli separated by 100 ms was measured. PPR was calculated as the ratio of the peak amplitude of $EPSC_2$/$EPSC_1$. Stimulus artifacts from the paired-pulse traces have been deleted. To measure evoked EPSCs, we performed whole-cell voltage clamp recording (at −60 mV) in presence of 100 μM picrotoxin (added to aCSF). A stimulating electrode was placed near the VMH (300–500 μm from the recording electrode) as mentioned above. The internal recording solution contained (in mM): $CsCH_3SO_3$ 125; CsCl 10; NaCl 5; $MgCl_2$ 2; EGTA 1; HEPES 10; (Mg)ATP 5; (Na)GTP 0.3 ; 10 lidocaine N-ethyl bromide (QX-314) (pH 7.35 with NaOH).

### Dendritic Spine Morphology

Cre-dependent adeno-associated viral vector AAV-DIO-mCherry was constructed by modifying the AAV-DIO-ChR2(H134R)-mCherry vector kindly provided by Dr. Karl Deisseroth (http://www.stanford.edu/group/dlab/optogenetics/sequence_info.html). Briefly, Asc1 and Nhe1 restriction sites were used to replace ChR2-mCherry fusion with mCherry alone (detailed methods in A.S. and B.L.S., unpublished data). The AAV-DIO-mCherry vector was then packaged into serotype 8 through the University of North Carolina Vector Core. AAV-mCherry virus (100 nl) at $1.5 \times 10^{12}$ viral mol/ml was then stereotaxically injected into the arcuate of AgRP-ires-Cre or POMC-Cre related animals at 4 weeks of age (as described above). 3 weeks later, animals were perfused and the brains were coronally sectioned at 30 μm thickness. Immunostaining against mCherry with rabbit anti-DsRed primary antibody (Clonetech; 1:2,500) and with Alex-594-anti-rabbit secondary antibody (Invitrogen) was then performed as previously described (Kong et al., 2010). Serial images of proximal dendritic structure labeled with mCherry immunoreactivity were taken under Zeiss confocal microscope (oil objective, 63×). In the coronal sections, primary dendrites or major secondary dendrites within a distance of ~150 μm from the soma that they originated from were imaged. These images were stacked using ImageJ software (1.44i version) for further analysis. The length of dendrites and diameter of spines were calculated according to the scale bars. Spine density was calculated by dividing total spine number to the length of the targeted dendrites.

### c-Fos in AgRP Neurons

Each day, for 12 days prior to sacrifice, the mice were acclimated to handling. For immunohistochemical detection of c-Fos and GFP in *Npy*-GFP mice and in *Agrp*-ires-Cre, *Grin1*$^{lox/lox}$, *Npy*-GFP mice, animals were sacrificed at 10 AM in either the ad lib fed state or after 24 hr of fasting (food removed at 10 AM on the previous day). The mice were perfused and brains were sectioned as described above. Assessment of c-Fos induction was performed using a previously developed method (Fuller et al., 2011) modified for colocalization with hrGFP in AgRP neurons. Brain sections were processed for immunohistochemical detection of c-Fos and hrGFP and counting.

Brain sections were washed in 0.1 M phosphate-buffered saline with Tween 20, pH 7.4 (PBST, 2 changes) and then incubated in the primary antiserum (rabbit polyclonal antibody agonist c-Fos, 1:150,000, AB-5, residues 4–17 from human c-Fos, Oncogene) for 2 days at room temperature. Sections were then washed in PBS and incubated in biotinylated secondary antiserum (Donkey anti-rabbit IgG, 1:1,000 in PBS, Jackson ImmunoResearch) for 2 hr, washed in PBS and incubated in avidin-biotin-horseradish peroxidase conjugate (Vector) for 2 hr. Sections were then washed again and incubated in a 0.06% solution of 3,3-diaminobenzidine tetrahydrochloride (DAB, Sigma) plus 0.02% $H_2O_2$.The sections were stained black with DAB by adding 0.05% cobalt chloride and 0.01% nickel ammonium sulfate. Sections were then washed extensively and incubated with chicken anti-GFP (1:1,000, Abcam) for 2 days at room temperature. Sections were then washed in PBS and incubated in biotinylated secondary antiserum (Donkey anti-chicken IgG, 1:1,000 in PBS, Jackson ImmunoResearch) for 2 hr, followed by a wash in PBS and incubation in avidin-biotin-horseradish peroxidase conjugate (Vector) for 2 hr. Sections were then washed again and incubated in a 0.06% solution of 3,3-diaminobenzidine tetrahydrochloride (DAB, Sigma) plus 0.02% $H_2O_2$. The sections were stained brown with DAB. Sections were then mounted, dried and stained with thionin, dehydrated and coverslipped. Cells in the section (−1.70 mm from bregma) were visualized and counted using a Zeiss microscope by an observer that was blinded to the condition or genotype of the mice. Data are expressed as the percentage of all AgRP neurons (i.e., all GFP-positive neurons) that were double-positive for c-Fos and GFP.

### Assessment of *Agrp*, *Npy*, *and Pomc* mRNAs

RNA was extracted from mouse hypothalami using STAT-60 Reagent (Isotex Diagnostics). cDNA was generated by reverse transcriptase (Clontech). *Agrp*, *Npy*, and *Pomc* were amplified from 0.5 ng of reverse-transcribed total RNA using TaqMan Universal PCR Mastermix (Applied Biosystems) with *Agrp*, *Npy*, and *Pomc* sense and antisense primers, and a dual-labeled probe (5′-FAM, 3′-TAMRA) (Applied Biosystems; assay on demand Mm00475829_g1, Mm00445771_m1, Mm00435874_m1, respectively). Standard curves were constructed by amplifying serial dilutions of cDNA (5 ng to 0.32 pg) and plotting cycle threshold (CT) values as a function of starting reverse-transcribed RNA. mRNA expression of *Agrp*, *Npy*, and *Pomc* was normalized to levels of the 18S ribosomal RNA housekeeping gene. Quantitative PCR was performed on Mx3000P instrument (Stratagene).

### Statistics

Statistical tests, as noted in the figure legends, were performed using Origin 8.0 (OriginLab, Northampton, MA).

## SUPPLEMENTAL INFORMATION

Supplemental Information includes three figures and can be found with this article online at doi:10.1016/j.neuron.2011.11.027.

## ACKNOWLEDGMENTS

We wish to thank M. Krashes, L. Vong, C. Bjorbaek, and J. Lu for helpful discussions; and B. Choi, X. Hu, S. Ma, and J. Yu for excellent technical support. This work was supported by grants from the National Institutes of Health (to B.B.L.: R01 DK089044, R01 DK071051, R37 DK053477, R01 DK075632, BNORC Transgenic Core-P30 DK046200 and BADERC Transgenic Core-P30 DK057521; to D.K.: a P&F from BADERC–P30 DK057521; to A.S.: F31 NS074842; to J.B.D.: K99 NS075136; to B.L.S.: NS046579) and the American Diabetes Association (to B.B.L.: Mentor-Based Postdoctoral Fellowship). A.S. is a recipient of a Shapiro predoctoral fellowship and J.B.D. is a recipient of a Parkinson's Disease Foundation postdoctoral fellowship (PDF-FBS-1106).

Accepted: November 22, 2011
Published: February 8, 2012

## REFERENCES

Aponte, Y., Atasoy, D., and Sternson, S.M. (2011). AGRP neurons are sufficient to orchestrate feeding behavior rapidly and without training. Nat. Neurosci. *14*, 351–355.

Balthasar, N., Coppari, R., McMinn, J., Liu, S.M., Lee, C.E., Tang, V., Kenny, C.D., McGovern, R.A., Chua, S.C., Jr., Elmquist, J.K., and Lowell, B.B. (2004). Leptin receptor signaling in POMC neurons is required for normal body weight homeostasis. Neuron *42*, 983–991.

Balthasar, N., Dalgaard, L.T., Lee, C.E., Yu, J., Funahashi, H., Williams, T., Ferreira, M., Tang, V., McGovern, R.A., Kenny, C.D., et al. (2005). Divergence of melanocortin pathways in the control of food intake and energy expenditure. Cell *123*, 493–505.

Belgardt, B.F., Okamura, T., and Brüning, J.C. (2009). Hormone and glucose signalling in POMC and AgRP neurons. J. Physiol. *587*, 5305–5314.

Bewick, G.A., Gardiner, J.V., Dhillo, W.S., Kent, A.S., White, N.E., Webster, Z., Ghatei, M.A., and Bloom, S.R. (2005). Post-embryonic ablation of AgRP neurons in mice leads to a lean, hypophagic phenotype. FASEB J. *19*, 1680–1682.

Bito, H. (2010). The chemical biology of synapses and neuronal circuits. Nat. Chem. Biol. *6*, 560–563.

Broberger, C., De Lecea, L., Sutcliffe, J.G., and Hökfelt, T. (1998). Hypocretin/orexin- and melanin-concentrating hormone-expressing cells form distinct populations in the rodent lateral hypothalamus: relationship to the neuropeptide Y and agouti gene-related protein systems. J. Comp. Neurol. *402*, 460–474.

Buchanan, K.A., Petrovic, M.M., Chamberlain, S.E., Marrion, N.V., and Mellor, J.R. (2010). Facilitation of long-term potentiation by muscarinic M(1) receptors is mediated by inhibition of SK channels. Neuron *68*, 948–963.

Butler, A.A., and Kozak, L.P. (2010). A recurring problem with the analysis of energy expenditure in genetic models expressing lean and obese phenotypes. Diabetes *59*, 323–329.

Castañeda, T.R., Tong, J., Datta, R., Culler, M., and Tschöp, M.H. (2010). Ghrelin in the regulation of body weight and metabolism. Front. Neuroendocrinol. *31*, 44–60.

Collingridge, G.L., Peineau, S., Howland, J.G., and Wang, Y.T. (2010). Long-term depression in the CNS. Nat. Rev. Neurosci. *11*, 459–473.

Cone, R.D. (2005). Anatomy and regulation of the central melanocortin system. Nat. Neurosci. *8*, 571–578.

Cowley, M.A., Smith, R.G., Diano, S., Tschöp, M., Pronchuk, N., Grove, K.L., Strasburger, C.J., Bidlingmaier, M., Esterman, M., Heiman, M.L., et al. (2003). The distribution and mechanism of action of ghrelin in the CNS demonstrates a novel hypothalamic circuit regulating energy homeostasis. Neuron *37*, 649–661.

Csakvari, E., Hoyk, Z., Gyenes, A., Garcia-Ovejero, D., Garcia-Segura, L.M., and Párducz, A. (2007). Fluctuation of synapse density in the arcuate nucleus during the estrous cycle. Neuroscience *144*, 1288–1292.

Dhillon, H., Zigman, J.M., Ye, C., Lee, C.E., McGovern, R.A., Tang, V., Kenny, C.D., Christiansen, L.M., White, R.D., Edelstein, E.A., et al. (2006). Leptin directly activates SF1 neurons in the VMH, and this action by leptin is required for normal body-weight homeostasis. Neuron *49*, 191–203.

Diano, S., Farr, S.A., Benoit, S.C., McNay, E.C., da Silva, I., Horvath, B., Gaskin, F.S., Nonaka, N., Jaeger, L.B., Banks, W.A., et al. (2006). Ghrelin controls hippocampal spine synapse density and memory performance. Nat. Neurosci. *9*, 381–388.

Engert, F., and Bonhoeffer, T. (1999). Dendritic spine changes associated with hippocampal long-term synaptic plasticity. Nature *399*, 66–70.

Frankfurt, M., Gould, E., Woolley, C.S., and McEwen, B.S. (1990). Gonadal steroids modify dendritic spine density in ventromedial hypothalamic neurons: a Golgi study in the adult rat. Neuroendocrinology *51*, 530–535.

Friedman, J.M. (2009). Leptin at 14 y of age: an ongoing story. Am. J. Clin. Nutr. *89*, 973S–979S.

Fuller, P.M., Sherman, D., Pedersen, N.P., Saper, C.B., and Lu, J. (2011). Reassessment of the structural basis of the ascending arousal system. J. Comp. Neurol. *519*, 933–956.

Giessel, A.J., and Sabatini, B.L. (2010). M1 muscarinic receptors boost synaptic potentials and calcium influx in dendritic spines by inhibiting postsynaptic SK channels. Neuron *68*, 936–947.

Gropp, E., Shanabrough, M., Borok, E., Xu, A.W., Janoschek, R., Buch, T., Plum, L., Balthasar, N., Hampel, B., Waisman, A., et al. (2005). Agouti-related peptide-expressing neurons are mandatory for feeding. Nat. Neurosci. *8*, 1289–1291.

Hahn, T.M., Breininger, J.F., Baskin, D.G., and Schwartz, M.W. (1998). Coexpression of Agrp and NPY in fasting-activated hypothalamic neurons. Nat. Neurosci. *1*, 271–272.

Higley, M.J., and Sabatini, B.L. (2008). Calcium signaling in dendrites and spines: practical and functional considerations. Neuron *59*, 902–913.

Huszar, D., Lynch, C.A., Fairchild-Huntress, V., Dunmore, J.H., Fang, Q., Berkemeier, L.R., Gu, W., Kesterson, R.A., Boston, B.A., Cone, R.D., et al. (1997). Targeted disruption of the melanocortin-4 receptor results in obesity in mice. Cell *88*, 131–141.

Kaelin, C.B., Xu, A.W., Lu, X.Y., and Barsh, G.S. (2004). Transcriptional regulation of agouti-related protein (Agrp) in transgenic mice. Endocrinology *145*, 5798–5806.

Kaiyala, K.J., and Schwartz, M.W. (2011). Toward a more complete (and less controversial) understanding of energy expenditure and its role in obesity pathogenesis. Diabetes *60*, 17–23.

Kerchner, G.A., and Nicoll, R.A. (2008). Silent synapses and the emergence of a postsynaptic mechanism for LTP. Nat. Rev. Neurosci. *9*, 813–825.

Kessels, H.W., and Malinow, R. (2009). Synaptic AMPA receptor plasticity and behavior. Neuron *61*, 340–350.

Kong, D., Vong, L., Parton, L.E., Ye, C., Tong, Q., Hu, X., Choi, B., Brüning, J.C., and Lowell, B.B. (2010). Glucose stimulation of hypothalamic MCH neurons involves K(ATP) channels, is modulated by UCP2, and regulates peripheral glucose homeostasis. Cell Metab. *12*, 545–552.

Krashes, M.J., Koda, S., Ye, C., Rogan, S.C., Adams, A.C., Cusher, D.S., Maratos-Flier, E., Roth, B.L., and Lowell, B.B. (2011). Rapid, reversible activation of AgRP neurons drives feeding behavior in mice. J. Clin. Invest. *121*, 1424–1428.

Kreitzer, A.C., and Malenka, R.C. (2008). Striatal plasticity and basal ganglia circuit function. Neuron *60*, 543–554.

Kwon, H.B., and Sabatini, B.L. (2011). Glutamate induces de novo growth of functional spines in developing cortex. Nature *474*, 100–104.

Luquet, S., Perez, F.A., Hnasko, T.S., and Palmiter, R.D. (2005). NPY/AgRP neurons are essential for feeding in adult mice but can be ablated in neonates. Science *310*, 683–685.

Malenka, R.C., and Nicoll, R.A. (1999). Long-term potentiation—a decade of progress? Science *285*, 1870–1874.

Maletic-Savatic, M., Malinow, R., and Svoboda, K. (1999). Rapid dendritic morphogenesis in CA1 hippocampal dendrites induced by synaptic activity. Science *283*, 1923–1927.

Parton, L.E., Ye, C.P., Coppari, R., Enriori, P.J., Choi, B., Zhang, C.Y., Xu, C., Vianna, C.R., Balthasar, N., Lee, C.E., et al. (2007). Glucose sensing by POMC neurons regulates glucose homeostasis and is impaired in obesity. Nature *449*, 228–232.

Pinto, S., Roseberry, A.G., Liu, H., Diano, S., Shanabrough, M., Cai, X., Friedman, J.M., and Horvath, T.L. (2004). Rapid rewiring of arcuate nucleus feeding circuits by leptin. Science *304*, 110–115.

Schnütgen, F., Doerflinger, N., Calléja, C., Wendling, O., Chambon, P., and Ghyselinck, N.B. (2003). A directional strategy for monitoring Cre-mediated recombination at the cellular level in the mouse. Nat. Biotechnol. *21*, 562–565.

Smart, J.L., Tolle, V., and Low, M.J. (2006). Glucocorticoids exacerbate obesity and insulin resistance in neuron-specific proopiomelanocortin-deficient mice. J. Clin. Invest. *116*, 495–505.

Sternson, S.M., Shepherd, G.M., and Friedman, J.M. (2005). Topographic mapping of VMH —> arcuate nucleus microcircuits and their reorganization by fasting. Nat. Neurosci. *8*, 1356–1363.

Takahashi, K.A., and Cone, R.D. (2005). Fasting induces a large, leptin-dependent increase in the intrinsic action potential frequency of orexigenic arcuate nucleus neuropeptide Y/Agouti-related protein neurons. Endocrinology *146*, 1043–1047.

Tong, Q., Ye, C.P., Jones, J.E., Elmquist, J.K., and Lowell, B.B. (2008). Synaptic release of GABA by AgRP neurons is required for normal regulation of energy balance. Nat. Neurosci. *11*, 998–1000.

Tsien, J.Z., Chen, D.F., Gerber, D., Tom, C., Mercer, E.H., Anderson, D.J., Mayford, M., Kandel, E.R., and Tonegawa, S. (1996a). Subregion- and cell type-restricted gene knockout in mouse brain. Cell *87*, 1317–1326.

Tsien, J.Z., Huerta, P.T., and Tonegawa, S. (1996b). The essential role of hippocampal CA1 NMDA receptor-dependent synaptic plasticity in spatial memory. Cell *87*, 1327–1338.

van den Pol, A.N. (2003). Weighing the role of hypothalamic feeding neurotransmitters. Neuron *40*, 1059–1061.

van den Pol, A.N., Yao, Y., Fu, L.Y., Foo, K., Huang, H., Coppari, R., Lowell, B.B., and Broberger, C. (2009). Neuromedin B and gastrin-releasing peptide excite arcuate nucleus neuropeptide Y neurons in a novel transgenic mouse expressing strong Renilla green fluorescent protein in NPY neurons. J. Neurosci. *29*, 4622–4639.

Vong, L., Ye, C., Yang, Z., Choi, B., Chua, S., Jr., and Lowell, B.B. (2011). Leptin action on GABAergic neurons prevents obesity and reduces inhibitory tone to POMC neurons. Neuron *71*, 142–154.

Xu, A.W., Kaelin, C.B., Morton, G.J., Ogimoto, K., Stanhope, K., Graham, J., Baskin, D.G., Havel, P., Schwartz, M.W., and Barsh, G.S. (2005). Effects of hypothalamic neurodegeneration on energy balance. PLoS Biol. *3*, e415.

Xu, Y., Jones, J.E., Kohno, D., Williams, K.W., Lee, C.E., Choi, M.J., Anderson, J.G., Heisler, L.K., Zigman, J.M., Lowell, B.B., and Elmquist, J.K. (2008). 5-HT2CRs expressed by pro-opiomelanocortin neurons regulate energy homeostasis. Neuron *60*, 582–589.

Xu-Friedman, M.A., and Regehr, W.G. (2004). Structural contributions to short-term synaptic plasticity. Physiol. Rev. *84*, 69–85.

Yang, Y., Atasoy, D., Su, H.H., and Sternson, S.M. (2011). Hunger states switch a flip-flop memory circuit via a synaptic AMPK-dependent positive feedback loop. Cell *146*, 992–1003.

Yaswen, L., Diehl, N., Brennan, M.B., and Hochgeschwender, U. (1999). Obesity in the mouse model of pro-opiomelanocortin deficiency responds to peripheral melanocortin. Nat. Med. *5*, 1066–1070.

Yuste, R. (2010). Dendritic Spines (Cambridge: The MIT Press).